https://doi.org/10.5194/essd-2026-373
Preprint. Discussion started: 14 July 2026

Open Access Earth System Science Data Discussions

The Integrated Multi-proxy Paleoclimate Database for the Northeastern Tibetan Plateau

Yu Li[1, 2], Hao Shang[1], Shiyi Yan[1], Zhansen Zhang[1], MingJun Gao[1], Tingting Xi[1], Jiarui Zhao[1], Wanchen Sun[1]
[1]College of Earth and Environmental Sciences, Lanzhou University, Lanzhou 730000, China
[2]Key Laboratory of Western China's Environmental Systems (Ministry of Education), Lanzhou University, Lanzhou 730000, China
Correspondence: Yu Li (liyu@lzu.edu.cn)

Abstract The Northeastern Tibetan Plateau (NETP) is an important region influenced by the interaction between the Asian monsoon and the Westerlies. Diverse paleoclimate archives, including sedimentary profiles, ice cores, tree rings, surface soils, and meteorological stations, record environmental changes across multiple temporal scales. However, differences in temporal resolution, chronological depth, and proxy sensitivity make direct comparisons among these archives difficult. We present a paleoclimate database for the NETP that integrates these records within a unified framework. The database includes 147 sedimentary profiles, 456 surface soil samples, 23 tree ring width index (RWI) chronologies, 5 ice core records, and data from 73 meteorological stations. The records were standardized using consistent chronological processing and proxy normalization methods to improve cross archive comparability. The database shows internal consistency among regional proxy records. The dataset combines the long term continuity of sedimentary profiles with the high-resolution climate signals preserved in tree rings and ice cores. In addition, integrating surface soil proxies with meteorological observations provides a modern calibration framework for evaluating proxy responses to temperature, precipitation, and elevation gradients. By linking geological archives with instrumental observations across multiple timescales, the dataset supports regional paleoclimate reconstruction and environmental change research in the NETP. The Integrated Multi-proxy Paleoclimate Database for the Northeastern Tibetan Plateau is available at https://doi.org/10.17632/cp7kftnb94.1 (Li, 2026)

1 Introduction

Quantitative reconstruction of past climate change relies on a variety of paleoclimate proxies archived in diverse natural records, including ice cores, tree rings, sedimentary sequences, surface soils, and modern meteorological observations. These archives provide climatic information ranging from interannual to multi-millennial scales, enabling comprehensive analyses of climate variability across multiple temporal dimensions. With the continuous accumulation of observational data, the integrated application of multi-proxy indicators combining multiple proxies is now a key focus in paleoclimate research. However, proxies form and respond differently to the environment, resulting in varying temporal resolutions, climatic

https://doi.org/10.5194/essd-2026-373
Preprint. Discussion started: 14 July 2026

meanings, and uncertainties. These differences limit dataset comparability and make integration difficult. This issue is especially prominent in regional studies involving complex environments.

As the highest plateau on Earth, the Tibetan Plateau (TP) is recognized as the "Third Pole" and an "amplifier of global climate change" (Pan et al., 1995; Wu et al., 2005; Qiu, 2008; Liu et al., 2009a)The Northeastern Tibetan Plateau (NETP) encompasses key geographical units, including the Qilian Mountains, the Qaidam Basin, the Hexi Corridor, and the Lanzhou section of the upper Yellow River. Notably, this region forms a critical intersection between the Asian monsoon and the Westerly jet stream. Such a unique climatic position provides distinct advantages for recording paleoclimatic evolution (Long et al., 2025; Li et al., 2025; Wang et al., 2026). Extensive research has established the NETP as one of the most mature regions globally for paleoclimate studies since the Last Glacial Maximum (LGM). It hosts the richest variety of proxy types in the global mid to high latitudes, including surface soils (Wang et al., 2017; Chen et al., 2020; Zan et al., 2022; Li and Peng, 2023), sedimentary profiles (Gasse et al., 1991; Liu et al., 2014; Wünnemann et al., 2010; Herzschuh et al., 2011; Kasper et al., 2012; Bird et al., 2014; Doberschutz et al., 2014; Hou et al., 2017a, 2017b; Conroy et al., 2017;), tree rings (Yang et al., 2012; Gou et al., 2013; He et al., 2013; Qie et al., 2022), and ice cores (Thompson et al., 1997; Yao et al., 1997). This dense network helps track spatial and temporal changes of climate elements.

Despite this data wealth, integrating these diverse carriers remains challenging. Meteorological stations provide high-precision modern records; tree rings offer clear interannual resolution; ice cores record long-sequence climatic information; and stratigraphic profiles provide continuous paleoenvironmental sequences over multi-millennial scales. These differences in spatio-temporal resolution make direct comparisons difficult. Also, differing proxy responses add to this complexity. For instance, early Holocene lacustrine carbonate $\delta^{18}O$ records from Lake Qinghai are typically interpreted as indicating increased effective moisture and a strengthened summer monsoon (Lister et al., 1991; Liu et al., 2007; An et al., 2012). However, lake-level proxies and paleoshoreline evidence from the same lake indicate a relatively dry climate during this period (Zhang et al., 1994; Liu et al., 2013; Wang et al., 2014; Liu et al., 2015). Holocene temperature variations also exhibit discrepancies between pollen-inferred early to mid Holocene warming (Tang et al., 1999, 2000, 2009; Herzschuh et al., 2006; Shen et al., 2008; Lu et al., 2011; Ma et al., 2014) and the mid Holocene cooling phase recorded by the Guliya ice core $\delta^{18}O$ (Thompson et al., 1997). To address these limitations,this study constructs a regional multi-proxy paleoclimate database for the NETP. By systematically integrating sedimentary profiles, surface soils, tree rings, ice cores, and meteorological observations, the database integrating these records unifies the diverse data sources. All sedimentary records were converted into a unified chronological sequence using age-depth models and interpolated to a consistent temporal resolution. Subsequently, Z-score normalization was applied to proxy indicators to eliminate dimensional effects. This framework allows for cross-proxy comparisons and quantitative analysis, and

https://doi.org/10.5194/essd-2026-373
Preprint. Discussion started: 14 July 2026

provides constraints for climate model validation.

2 Study region

The study region is located on the Northeastern Tibetan Plateau (98.0°-103.5°E, 32.7°-38.2°N), situated in the transition zone between China's first and second topographic steps, encompassing typical geographical units such as the Qaidam Basin, the Hexi Corridor, the Lanzhou section of the upper Yellow River, and the Qilian Mountains (Fig. 1). Regional elevation generally ranges between 2 and 4 km and gradually rises from the basins and corridor areas to over 5000 m in the mountains, forming a significant vertical altitudinal gradient. The complex terrain causes high spatial variation in sedimentary and hydrological systems. It also creates gaps in the climate records in the paleoclimatic information recorded by various carriers. The NETP is jointly influenced by the East Asian Summer Monsoon (EASM), the Indian Summer Monsoon (ISM), and the Westerly circulation, making it extremely sensitive to global changes (Ding and Wang, 2005; Schiemann et al., 2009; Chen et al., 2020; Huang et al., 2020; Li et al., 2022). Since the Late Glacial, the interplay and fluctuation of these different circulation systems have resulted in strong spatio-temporal asymmetry in regional hydrothermal configurations. This increases the uncertainty of single-proxy reconstructions and complicates data integration across different terrains.

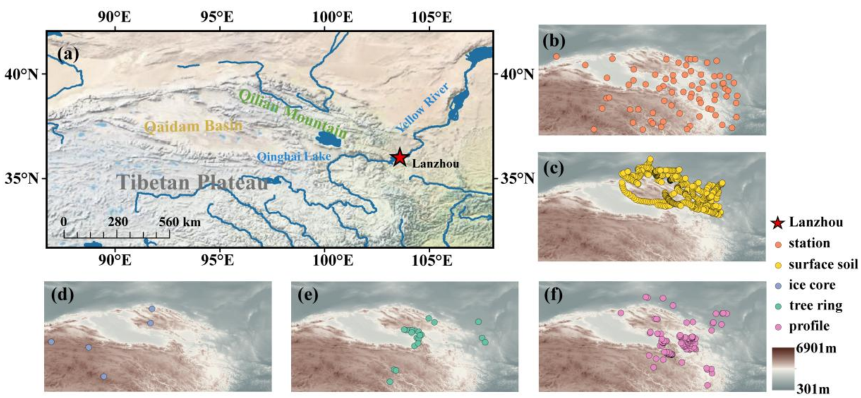

Figure 1. Spatial distribution of multi-proxy climate records in theNortheastern Tibetan Plateau. (a) Extent and geographical units of the Northeastern Tibetan Plateau (NETP); (b-f) spatial distribution of meteorological stations, surface soils, ice cores, tree rings, and sedimentary profiles integrated in this database.

3 Data compilation and processing

3.1 Data compilation

This study integrates five categories of data: sedimentary profiles, surface soil samples, tree ring records, ice core records, and meteorological stations (Tab. 1). This database covers timescales from modern observations to millennia and includes various physical and geochemical proxies. Sedimentary profile data were acquired through systematic literature searches across databases including Web of Science,

https://doi.org/10.5194/essd-2026-373
Preprint. Discussion started: 14 July 2026

Elsevier, CNKI, and Google Scholar, with studies containing original chronological information specifically selected. A total of 147 profiles were integrated, including metadata such as location, elevation, depth, and dating materials. This yielded a compilation of 1,006 chronological data points and multi-proxy sequences, including grain size, total organic carbon (TOC), magnetic susceptibility, C/N, $\delta^{13}C$, $\delta^{18}O$, as well as carbonates, silicates, and Rb/Sr ratios. Surface soil data were derived from field sampling and laboratory analysis, comprising 456 samples with location and elevation information, providing records of grain size, C/N ratios, and 289 carbon and oxygen stable isotope values. tree ring data were obtained from the NOAA database, consisting of 23 tree ring width index (RWI) chronologies, along with information on tree species and their distributions. Ice core data integrate five records from Dunde, Malan, Tanggula, Muztagh, and Laohugou, sourced from the NOAA, China Tibetan Plateau Data Center (TPDC) and published literature, providing $\delta^{18}O$ sequences and selected ionic proxies. Meteorological observation data were sourced from NOAA, containing temperature and precipitation records from 73 stations for the period 1973-2025.

Proxy type	Number of records	Temporal coverage (CE)	Spatial coverage	Elevation range (m)	Parameters
Station	73	1973-2025	32.20-39.00°N、85.60-105.00°E	609-4877	MAT, MAP
Surface soil	456	-	36.17-41.35°N、94.3-103.64°E	1037-4158	grain size, $\delta^{13}C_{org}$, $\delta^{18}O$, C/N, temperature , precipitation
Ice core	5	520-2010	33.11-39.43°N、87.179-96.57°E	5049-5750	$\delta^{18}O$, $C_2O_4^{2-}$, SO_4^{2-}, Ca^{2+}
Tree ring	23	-336-2020	32.66-38.57°N、95.72-108.90°E	1050-4324	RWI
Profile	147	-28050-2025	32.33-41.89°N、94.00-104.00°E	892-5133	grain size, TOC, magnetic susceptibility, C/N, $\delta^{13}C$, $\delta^{18}O$, OM, $CaCO_3$, carbonates, silicates , Rb/Sr

Table 1. Dataset Overview

3.2 Data processing

3.2.1 Processing of sedimentary records

This study compiled 1,006 published dating records to establish temporal frameworks for the sedimentary profiles. Radiocarbon dates were calibrated to calendar ages using the IntCal20 calibration curve. The median probability age was used as the chronological control point. For optically stimulated luminescence (OSL) records, the original text data were cleaned to extract representative age values. To reduce the influence of possible depositional disturbance, age inversions were

https://doi.org/10.5194/essd-2026-373
Preprint. Discussion started: 14 July 2026

Open Access Earth System Science Data Discussions

identified and excluded before further processing. All original dating information and uncertainties were preserved in the released database. The retained dating points were used to establish approximate age-depth relationships for each profile. Simple fitted relationships, including linear and low-order polynomial functions, were applied to support temporal interpolation and alignment among different records. Because the compiled profiles contain different dating methods and uneven chronological resolution, the fitted relationships were intended to provide generalized temporal support rather than high-precision chronologies. The fitted results do not replace the original dating data, which remain fully available in the released database. To support comparisons among different profiles, all proxy records were converted from the depth domain to the time domain. Each sequence was resampled at 50-year intervals to achieve a uniform temporal resolution. The corresponding depths for target ages were calculated using the fitted age-depth relationships. Proxy values were then obtained through linear interpolation. This procedure generated evenly spaced time series for subsequent regional analyses. A total of 45 profiles with relatively complete records and continuous proxy data were selected for integrated analysis. Each proxy sequence was standardized independently using Z-score normalization based on its own mean and standard deviation (Fig. 2). Ensemble statistics were then calculated for the standardized records at the same time intervals, including regional means and standard deviations. These results were used to describe overall environmental variability and data dispersion across the study region.

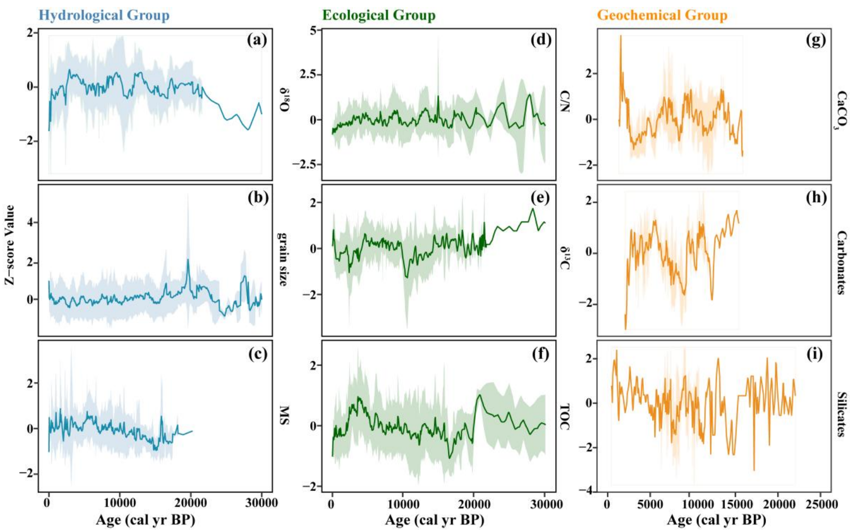

Figure 2. Standardized proxy time series from sedimentary records

3.2.2 Processing of surface soil dataset

Surface soil data in this study were collected from 456 sampling sites across various altitudinal and environmental gradients to ensure regional representativeness. All samples were processed and analyzed at the Key Laboratory of Western China's Environmental Systems (Ministry of Education), Lanzhou University. Grain size analysis was performed using a Malvern Mastersizer 2000 laser diffraction particle

https://doi.org/10.5194/essd-2026-373
Preprint. Discussion started: 14 July 2026

size analyzer, with a measurement range of 0.02-2000 μm and a repetitive error restricted to within 3%. The Carbon to Nitrogen (C/N) ratio was calculated by measuring organic carbon (OC) and total nitrogen (TN) contents via an elemental analyzer. Stable carbon and oxygen isotopic compositions were determined using an isotope ratio mass spectrometer (IRMS), with $\delta^{13}C_{org}$ and $\delta^{18}O$ values calibrated against the Vienna Pee Dee Belemnite (VPDB) and Vienna Standard Mean Ocean Water (VSMOW) standards, respectively. Additionally, the corresponding Mean Annual Temperature (MAT) and Mean Annual Precipitation (MAP) for each sampling site were obtained through spatial matching.

3.2.3 Processing of ice core records

This study integrated five ice core records from Dunde, Malan, Tanggula, Muztagh, and Laohugou, sourced from the National Oceanic and Atmospheric Administration (NOAA) and published literature. Significant variations exist in the temporal coverage and resolution among these records; the Dunde ice core provides the longest temporal span but with a decadal raw resolution, whereas the Tanggula and Muztagh cores consist of annual-resolution data. Records for the Malan and Laohugou cores were derived from published studies. For sequences sourced from literature with inconsistent resolutions, linear interpolation was applied to unify the data to an annual scale. The processed ice core data preserve their original variation patterns under a unified temporal scale.

3.2.4 Processing of tree ring and instrumental data

Tree ring data were retrieved from the NOAA public database, consisting of tree ring width index (RWI) chronologies within the study area at an annual resolution. The RWI sequences used in this study were the standardized products provided by the database, and no additional processing was performed. Meteorological observation data were likewise obtained from NOAA, encompassing daily temperature and precipitation records from 73 stations in the study area from 1973 to 2025. The original units were converted from Fahrenheit and inches to Celsius and millimeters, respectively, to ensure data consistency and comparability. Daily observations were aggregated into annual sequences.

4 Results and discussions

4.1 Proxy relationships

Sedimentary profiles provide continuous, multi-proxy records for reconstructing paleoclimates. (Chen et al., 2020). Organic geochemical proxies and micro-biomarkers in lacustrine sediments can reconstruct the evolution of regional ecosystem productivity, large oscillations in summer temperatures, and the temperature-driven drying processes in inland basins (Hou et al., 2016; Wu et al., 2020). Physical characteristics in aeolian and loess strata are vital indicators for tracking dust transport dynamics, the intensity evolution of the East Asian winter monsoon, and the history of regional aeolian desertification (Lehmkuhl et al., 2014; Li and Morrill, 2015; Hu et al., 2017, 2018).

Correlation analysis (Fig. 3) based on profile data with multi-proxy records demonstrates the statistical relationships among different proxy indicators and their

https://doi.org/10.5194/essd-2026-373
Preprint. Discussion started: 14 July 2026

associations with geographical factors. Correlation strengths vary, showing inconsistent links between proxies. Among geographical factors, elevation exhibits relatively strong negative correlations with both latitude and longitude, with the corresponding scatter distributions showing an overall downward trend; however, the point distributions still possess a certain degree of dispersion and do not present a strictly linear relationship. $\delta^{18}O$ exhibits a significant negative correlation with grain size. Furthermore, $\delta^{18}O$ shows significant positive correlations with TOC and C/N, characterized by relatively concentrated scatter distributions. Magnetic susceptibility (MS) presents relatively significant negative correlations with $\delta^{13}C$, $\delta^{18}O$, longitude, and latitude, with its scatter distributions being relatively dispersed. In contrast, $\delta^{18}O$, TOC, and C/N exhibit weak correlations with environmental factors, including elevation, longitude, and latitude.

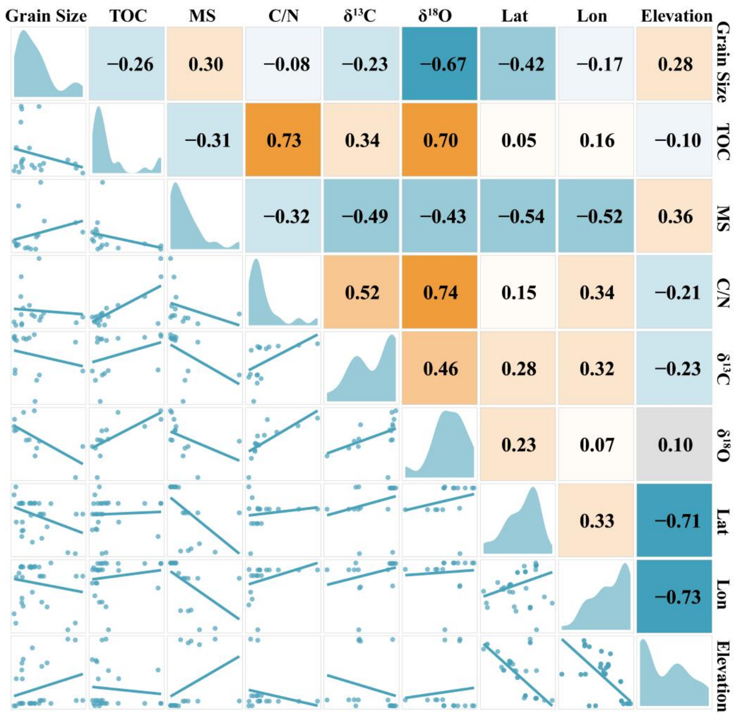

Figure 3. Correlation among proxy variables and geographic factors. (Note: MS denotes magnetic susceptibility.)

4.2 Temporal characteristics

Ice cores provide strong sedimentary continuity, high dating precision, and the coexistence of multiple proxy indicators, constitute crucial data for multi-timescale environmental reconstructions on the Tibetan Plateau (Cheng, 2026). $\delta^{18}O$ tracks the regional water cycle and helps delineate the boundary of influence between the Asian summer monsoon and the Westerlies (Tian et al., 2001; Wang et al., 2006). Pollen assemblages and specific chemical microparticles preserved in ice cores show past regional vegetation changes and surface material emissions (Liu et al., 1998; Cui et al.,

https://doi.org/10.5194/essd-2026-373
Preprint. Discussion started: 14 July 2026

Open Access Earth System Science Data Discussions

2011a; Cui et al., 2011b). As shown in Fig. 4, the five ice core sequences (Dunde, Malan, Muztagh, Tanggula, and Laohugou) integrated in this dataset can be classified based on their temporal coverage. Dunde and Malan represent long timescale records; Muztagh and Tanggula provide centennial scale observations; while Laohugou serves as a high-resolution, 46-year short sequence. Across all records, Large $\delta^{18}O$ variations across all records indicate strong climate fluctuations. The long-timescale cores distinctly capture historical cold phases likely corresponding to the Little Ice Age (LIA). The Dunde ice core exhibits pronounced $\delta^{18}O$ depletion during the 14th and 17th centuries. The Malan sequence records a more severe cooling episode, with values plunging to an absolute minimum of -18.3 in the 1790s. The Malan record also displays the widest isotopic range (-18.3 to -7.9), reflecting extreme climate fluctuations. In the 20th century, the records show different trends. The Malan sequence exhibits a continuous, long-term warming trajectory from 1900 to 1994. The Dunde record peaked in the 1940s before experiencing a reversal in the 1960s and 1970s. This mid to late 20th-century cooling phase is concurrently recorded as distinct low-value troughs in both the Muztagh and Tanggula centennial sequences between the 1950s and 1970s. In recent decades, multiple cores indicate an intensified warming signal, marked by positive $\delta^{18}O$ anomalies in the Muztagh and Tanggula records during the early 2000s. The short Laohugou sequence captures extremeenvironmental events. Its $C_2O_4^{2-}$ concentrations generally remained at low background levels, but showed sudden spikes in 1982, 1987, and 2004. These peaks suggest sudden environmental events.

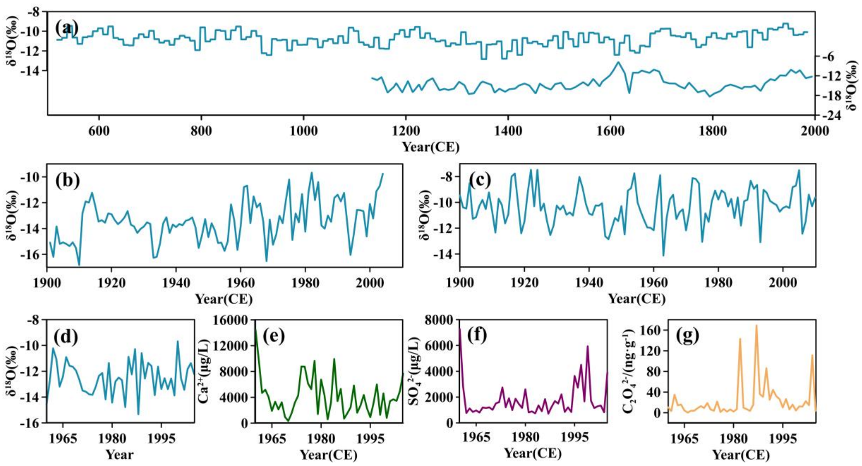

Figure 4. Multi-timescale ice core proxy records. (a) Long timescale Dunde and Malan ice cores; (b-c) medium timescale Tanggula and Muztagh ice cores; (d-g) short timescale Laohugou ice core.

Tree rings provide precise interannual resolution and are highly sensitive to environmental changes. This makes them key proxies for reconstructing the climate of the Northeastern Tibetan Plateau over the past millennium. (Hou et al., 1999). However, the response relationship between radial tree growth and climatic elements is not singular. It is driven by interactions between climate and species-specific traits.

https://doi.org/10.5194/essd-2026-373
Preprint. Discussion started: 14 July 2026

Even within the same type of habitat, the climate signals captured by different tree species exhibit significant differences: for instance, in the eastern Qilian Mountains, the ring width of Qilian juniper primarily responds to temperature fluctuations, whereas Qinghai spruce is more sensitive to precipitation changes (Zhan et al., 2019). Furthermore, the climate response patterns of the same tree species diverge across different altitudinal and latitudinal gradients (Liang et al., 2010; Yang et al., 2013). This sensitivity rule has allowed tree ring width to be widely and successfully applied in reconstructing regional large-scale precipitation fluctuations (Gou et al., 2013; He et al., 2013), historical runoff inversion (Liu et al., 2009b; Yang et al., 2012), and the precise identification of extreme flood events (Qie et al., 2022). This dataset includes 23 high quality RWI chronologies to capture these complex responses (Fig. 5). High altitude Qilian juniper sequences provide long and stable climate signals. Low altitude Chinese pine sequences are highly sensitive to abrupt local environmental changes. Under a unified annual resolution framework, Qilian juniper sampling sites distributed in high-altitude regions generally possess ultra-long temporal coverages ranging from hundreds to thousands of years, which is attributed to the extreme natural longevity of this species (Yang et al., 2014; Zhang et al., 2014; Yin et al., 2016). High altitude Qilianshan juniper chronologies exhibit relatively stable radial growth trajectories. Their RWI series demonstrate low-amplitude variance and attenuated low-frequency fluctuations. Conversely, low altitude Chinese pine sequences are characterized by pronounced interannual volatility, with their RWI series displaying extreme positive and negative anomalies. Statistical evaluation reveals that the variance amplitude of the pine chronologies is approximately three times that of the juniper records. This indicates that low altitude forest ecosystems are sensitive to short term, localized hydroclimatic extremes. In contrast, the dampened variance of the high altitude juniper sequences more reliably captures long term, large scale regional climate forcing.

https://doi.org/10.5194/essd-2026-373
Preprint. Discussion started: 14 July 2026

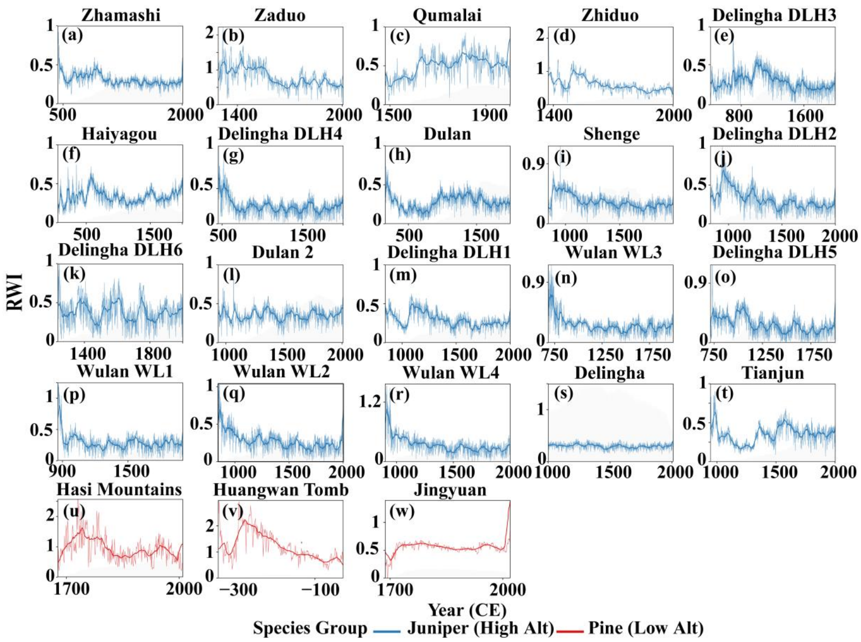

Figure 5. tree ring width index (RWI) chronologies across elevation gradients. (a-t) RWI chronologies of Qilian juniper (Sabina przewalskii Kom.) from high-altitude regions in the Northeastern Tibetan Plateau (NETP); (u-w) RWI chronologies of Chinese pine (Pinus tabuliformis Carrière) from low-altitude regions in the NETP.

4.3 Modern observations and proxy context

Station records and surface soils form the modern baseline for this database. (Shi et al., 2022). Comparing surface soil proxies with station data reveals how sedimentary proxies respond to regional climate gradients. (Li and Peng, 2023; Wang et al., 2017). In the monsoon marginal zone, the significant positive correlation between surface soil magnetic characteristics and station-observed precipitation helps delineate the boundaries between semi arid and arid climates (Zan et al., 2022). The spatial heterogeneity of surface soil grain-size distributions clearly records the interaction between modern weathering dynamics and local hydrological processes (Chen et al., 2020). However, in extremely arid inland interiors, some soil proxies do not match precipitation records, suggesting that non climatic factors must be fully considered when interpreting proxy records in specific environments (Huo et al., 2025). This calibration validates the proxies and provides a modern baseline to isolate non-climatic noise for calibrating high-resolution records. (Li and Peng, 2023; Wang et al., 2017). Surface soil data (Fig. 6) quantitatively characterize the statistical relationship structure between proxy indicators and modern climatic variables and topographic factors. From the regression results, the C/N ratio exhibits a significant negative correlation with precipitation, a weak positive correlation with temperature, and a weak correlation with elevation, indicating variations in its response intensity to different climatic variables. Grain size displays consistent trends across three dimensions: decreasing with increasing elevation, decreasing with increasing

https://doi.org/10.5194/essd-2026-373
Preprint. Discussion started: 14 July 2026

Open Access Earth System Science Data Discussions

precipitation, and increasing with increasing temperature. $\delta^{13}C$ is negatively correlated with precipitation, while exhibiting weak relationships with temperature and elevation; the correlation of $\delta^{18}O$ across all variable directions is generally low . Regarding distribution characteristics, the sampling sites are primarily concentrated in two high-density intervals—temperatures of 5-10 °C, precipitation of 50-150 mm, and elevations of 1000-1500 m and 3000-3500 m—revealing a distinct spatial stratification structure. In the scatter distributions, most data points cluster around the regression trends, with a limited proportion of outliers, indicating the overall stability of the statistical relationships.

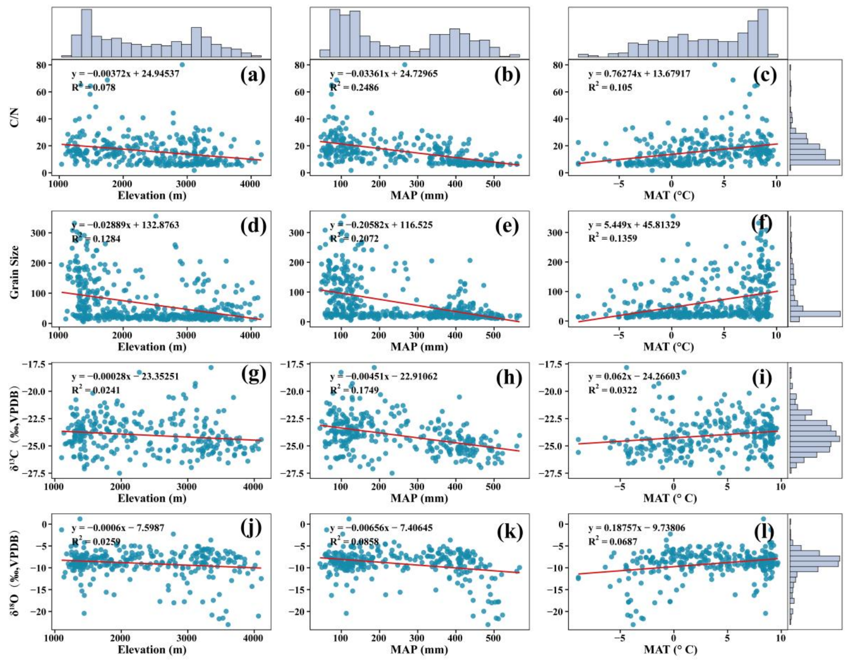

Figure 6 Surface soil proxy-environment relationships

Meteorological station data provide modern climate baselines (Fig. 7). The stations are primarily distributed within the altitudinal range of 2600-3500 m, with spatial coverage concentrated in the mid to high altitude zones. Z-score heatmaps based on 200 m elevation bins and 3-year averages indicate that temperature was dominated by negative anomalies during most periods, with the extent of positive anomalies expanding significantly after 2015; during the same period, precipitation also exhibited episodic characteristics of transitioning from negative to positive anomalies. Different altitudinal zones displayed similar anomaly signs during the same periods, although their intensities varied.

In the multi-archive comparison (Fig. 7_d), the Muztagata ice core $\delta^{18}O$ and tree ring width indices (RWI) provide medium to long timescale information (1900-1980), while the precipitation data recorded by stations cover the modern stage (1973-2025). Since high original ice core $\delta^{18}O$ values indicate arid environments, which physically contrasts with the humid conditions indicated by high RWI and instrumental

https://doi.org/10.5194/essd-2026-373
Preprint. Discussion started: 14 July 2026

Open Access Earth System Science Data Discussions

precipitation, the $\delta^{18}O$ sequence was uniformly multiplied by -1 to facilitate direct comparison.After unifying the environmental indications, the overall variation trends of the δ18O and RWI between 1900 and 1980 are similar, showing a downward trend during 1913-1919 and 1961-1967, and an upward trend during 1967-1969. However, these two paleoclimate sequences demonstrated pronounced opposite trends during the 1920s and 1930s. Furthermore, a comparison of their fluctuation characteristics reveals that the overall variations of the RWI generally lag the $\delta^{18}O$ sequence by approximately 4 to 5 years.During the overlapping period with station precipitation data (1973-1980), the RWI, $\delta^{18}O$, and station precipitation data maintained consistency in their overall variation trends. This trend consistency during the overlapping period establishes an effective temporal calibration, logically allowing the variations of paleoclimate proxies to extend into modern instrumental records. Beyond the splicing of time series, the sedimentary profile and topsoil (Fig. 3) further perfect the continuous record of regional environmental evolution. On this basis, the co-variation of multiple profile proxies within a unified temporal framework reflects the integrated response of this record to multiple environmental factors.

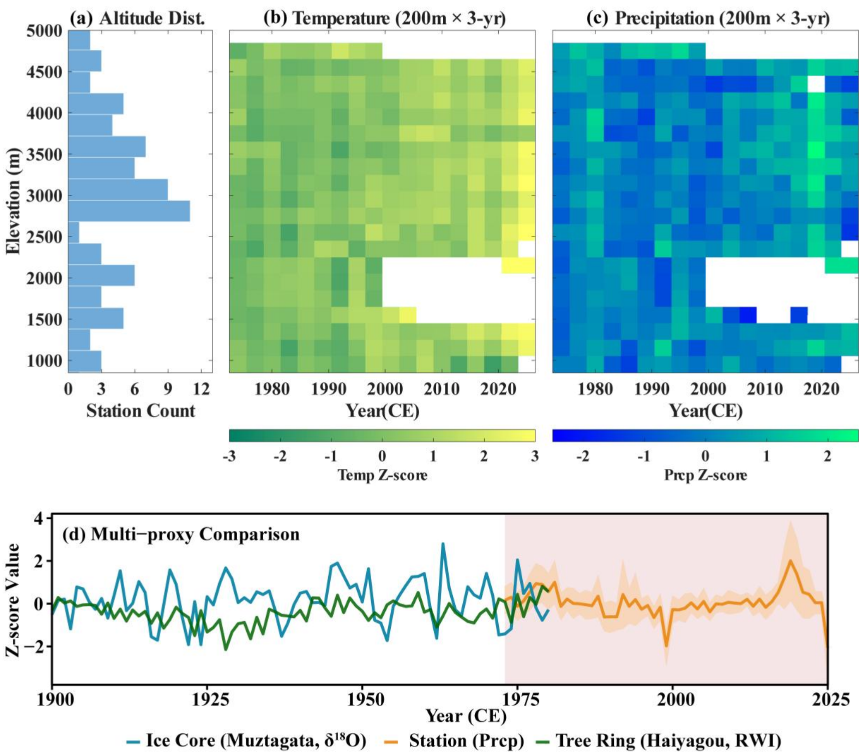

Figure 7. Modern observations and cross-archive continuity. (a) Histogram of station distribution across elevation gradients; (b-c) Heatmaps showing the spatiotemporal variations of station-observed temperature and precipitation across elevation and time; (d) Comparison of multi-archive proxies including ice core, tree ring, and meteorological stations, where the orange line represents the standardized (Z-score)

multi-year precipitation observations from stations.

4.4 Challenges and future directions of paleoclimate research in the NETP

Integrating diverse records in the NETP is challenging due to inherent differences in temporal resolution. Meteorological station data and tree rings provide precise annual or sub-annual records. In contrast, ice cores and sedimentary profiles generally reflect decadal to centennial variations. Furthermore, surface soil samples primarily offer modern spatial baselines rather than continuous time series. Disparities in chronological control methods across different archives further complicate integration. Sedimentary profiles rely on radiocarbon (AMS ^{14}C) and optically stimulated luminescence (OSL) dating to establish age-depth models, tree ring sequences provide absolute chronological constraints through cross-dating, and ice core records are calibrated based on layer counting or numerical modeling. The inherent differences in precision and uncertainty estimation among these methods may lead to temporal offsets or inconsistencies across multiple sequences (Reimer et al., 2020; Bronk Ramsey, 2009). At the proxy level, parameters such as $\delta^{18}O$, grain size, and C/N ratios respond to hydrological processes and associated climatic conditions; however, their numerical ranges and environmental sensitivities vary, which may introduce additional uncertainties during the unified standardization process, particularly in cross regional or altitudinal comparisons (Bradley, 2015).Spatially, constrained by accessibility and preservation conditions in high-altitude terrain, existing data tend to cluster in more accessible river valleys or piedmont areas, resulting in a relative paucity of sampling sites in high-altitude transition zones and key watersheds. This limits our ability to map temperature and precipitation gradients. Regarding modern observations, although meteorological station records provide high temporal resolution, their coverage is primarily limited to recent decades, exhibiting only narrow overlap with tree ring and ice core records. This restricts comparisons to short time windows and limits the direct validation of long-term variations (PAGES 2k Consortium, 2017).

This multi-archive dataset integrates records by standardizing diverse proxies into a single framework. Future research necessitates higher-resolution sampling in key regions to reduce discrepancies in temporal intervals, alongside improvements in age-modeling and uncertainty quantification to enhance temporal alignment precision across sequences. Furthermore, with the advancement of data assimilation and machine learning, coupling multi-source proxy data with climate models has become a pivotal direction for exploring proxy relationships (Hakim et al., 2016; Dee et al., 2016). The continuous optimization of sampling resolution, chronological frameworks, and proxy systems, as well as the systematic integration of multi-archive data within a unified framework can enhance the development of paleoclimate research in this region.

5 Data availability

The Integrated Multi-proxy Paleoclimate Database for the Northeastern Tibetan Plateau is now publicly available, and the data can be found at https://doi.org/10.17632/cp7kftnb94.1 (Li, 2026)

6 Conclusion

This study constructs the Integrated Multi-proxy Paleoclimate Database for the Northeastern Tibetan Plateau integrating sedimentary profiles, surface soils, tree rings, ice cores, and meteorological stations under a unified chronological and Z-score standardized framework. Integration of multiple archives differentiates climate signals across timescales. Sedimentary profiles provide continuous sequences on a millennial scale. Deep ice cores and high altitude tree rings track low frequency background shifts. Short ice core records and low altitude tree rings capture high frequency environmental extremes. Cross validation between surface soils and modern meteorological stations establishes a spatial calibration baseline. This clarifies the sensitivity of proxy indicators to temperature, precipitation, and elevation gradients. By bridging geological archives with instrumental observations, this database provides fundamental data for regional multiple proxy comparisons and multiple timescale paleoclimate reconstructions. This integrated dataset provides a long term benchmark for understanding environmental evolution in this sensitive global climate change amplifier. Furthermore, these standardized records offer critical observational constraints for validating paleoclimate models and predicting regional climate dynamics.

Author contributions. YL: conceptualization and investigation. HS: data collection, data processing and writing (original draft preparation). SY: methodology and writing (reviewing and editing). ZZ and MG: software and data curation. TX, JZ, and WS: validation and resources.

Competing interests. The contact author has declared that none of the authors has any competing interests.

Acknowledgements.
We wish to thank the editor and the anonymous reviewers for providing critical and valuable comments that helped to improve the paper. We thank all of the researchers and institutions that provided data. During the preparation of this manuscript, we used Gemini 3 to improve readability. After using this service, we carefully and thoroughly reviewed and revised the content as necessary. We take full responsibility for the integrity and accuracy of the publication.

Financial support. This research was supported by the National Natural Science Foundation of China (42371159).

References

An, Z., Colman, S. M., Zhou, W., Li, X., Brown, E. T., Jull, A. J. T., Cai, Y., Huang, Y., Lu, X., Chang, H., Song, Y., Sun, Y., Xu, H., Liu, W., Jin, Z., Liu, X., Cheng, P., Liu, Y., Ai, L., Li, X., Liu, X., Yan, L., Shi, Z., Wang, X., Wu, F., Qiang, X., Dong, J., Lu, F., and Xu, X.: Interplay between the westerlies and asian monsoon

https://doi.org/10.5194/essd-2026-373
Preprint. Discussion started: 14 July 2026

recorded in lake Qinghai sediments since 32 ka, Sci. Rep., 2, 619, https://doi.org/10.1038/srep00619, 2012.

Bird, B. W., Polisar, P. J., Lei, Y., Thompson, L. G., Yao, T., Finney, B. P., Bain, D. J., Pompeani, D. P., and Steinman, B. A.: A Tibetan lake sediment record of Holocene Indian summer monsoon variability, Earth Planet. Sci. Lett., 399, 92-102, https://doi.org/10.1016/j.epsl.2016.09.004, 2014.

Bradley, R. S.: Paleoclimatology: Reconstructing Climates of the Quaternary, 3rd edn., Academic Press, 2015.

Bronk Ramsey, C.: Bayesian analysis of radiocarbon dates, Radiocarbon, 51, 337-360, https://doi.org/10.1017/S0033822200033865, 2009.

Chen, F., Zhang, J., Liu, J., Cao, X., Hou, J., Zhu, L., Xu, X., Liu, X., Wang, M., Wu, D., Huang, L., Zeng, T., Zhang, S., Huang, W., Zhang, X., and Yang, K.: Climate change, vegetation history, and landscape responses on the Tibetan Plateau during the Holocene: A comprehensive review, Quat. Sci. Rev., 243, 106444, https://doi.org/10.1016/j.quascirev.2020.106444, 2020.

Cheng, H.: The age of ice cores from Qinghai-Xizang Plateau, Chin. Sci. Bull., https://doi.org/10.1360/CSB-2025-5593, 2026.

Conroy, J. L., Hudson, A. M., Overpeck, J. T., Liu, K., Wang, L., and Cole, J. E.: The primacy of multidecadal to centennial variability over late-Holocene forced change of the Asian Monsoon on the southern Tibetan Plateau, Earth Planet. Sci. Lett., 458, 337-348, https://doi.org/10.1016/j.epsl.2016.10.044, 2017.

Cui, X., Ren, J., Qin, X., Du, W., Sun, W., Yu, G., Wang, Z., Wang, X., Sun, W., and Wang, Y.: Climatic and Environmental Records within a Shallow Ice Core at Laohugou Glacier No.12, Qilian Mountains, J. Glaciol. Geocryol., 33, 1251-1258, https://doi.org/10.7522/j.issn.1000-0240.2011.0171, 2011a (in Chinese).

Cui, X., Ren, J., Qin, X., Yu, G., Liu, W., and Xie, A.: Oxalate, fluoride record and their environmental significance in Laohugou Glacier 12 Qilian Mountains, Environ. Chem., 30, 1919-1925, https://www.sciengine.com/EC/articleIndex?doi=10.0000/j.0254-6108.2011301119191925&scroll=, 2011b (in Chinese).

Dee, S. G., Steiger, N. J., Emile-Geay, J., and Hakim, G. J.: On the utility of proxy system models for estimating climate states over the Common Era, J. Adv. Model. Earth Syst., 8, 1164-1179, https://doi.org/10.1002/2016MS000677, 2016.

Ding, Q. and Wang, B.: Circumglobal teleconnection in the northern hemisphere summer, J. Climate, 18, 3483-3505, https://doi.org/10.1175/jcli3473.1, 2005.

Doberschutz, S., Frenzel, P., Haberzettl, T., Kasper, T., Wang, J., Zhu, L., Daut, G., Schwalb, A., and Mausbacher, R.: Monsoonal forcing of Holocene paleoenvironmental change on the central Tibetan Plateau inferred using a sediment record from Lake Nam Co (Xizang, China), J. Paleolimnol., 51, 253-266, https://doi.org/10.1007/s10933-013-9702-1, 2014.

Gasse, F., Arnold, M., Fontes, J. C., Fort, M., Gibert, E., Huc, A., Li, B., Li, Y., Liu, Q., and Melieres, F.: A 13,000-year climate record from western Tibet, Nature, 353, 742-745, https://doi.org/10.1038/353742a0, 1991.

Gou, X., Yang, T., Gao, L., Deng, Y., Yang, M., and Chen, F.: A 457-year reconstruction of precipitation in the southeastern Qinghai Tibet Plateau, China using tree-ring records, Chin. Sci. Bull., 58, 978-985, https://doi.org/10.1007/s11434-012-5539-7, 2013 (in Chinese).

Hakim, G. J., Emile-Geay, J., Steig, E. J., et al.: The Last Millennium Climate Reanalysis project: Framework and first results, J. Geophys. Res.-Atmos., 121, 6745-6764, https://doi.org/10.1002/2016JD024751, 2016.

He, M., Yang, B., Bräuning, A., Wang, J., and Wang, Z.: Tree-ring derived millennial precipitation record for the south-central Tibetan Plateau and its possible driving mechanism, Holocene, 23, 36-45, https://doi.org/10.1177/0959683612450198, 2013.

Herzschuh, U.: Palaeo-moisture evolution in monsoonal Central Asia during the last 50,000 years, https://doi.org/10.1016/j.quascirev.2005.02.006, Quat. Sci. Rev., 25, 163-178, 2006.

Herzschuh, U., Ni, J., Birks, H. J. B., and Böhner, J.: Driving forces of mid-Holocene vegetation shifts on the upper Tibetan Plateau, with emphasis on changes in atmospheric CO_2 concentrations, https://doi.org/10.1016/j.quascirev.2011.03.007, Quat. Sci. Rev., 30, 1907-1917, 2011.

Hou, A., Peng, S., and Zhou, G.: The study of the reactions of tree rings to the climate change and its applications, Ecol. Sci., 18, 16-23, https://doi.org/10.3969/j.issn.1008-8873.1999.03.004, 1999 (in Chinese).

Hou, J., D'Andrea, W. J., Wang, M., He, Y., and Liang, J.: Influence of the Indian monsoon and the subtropical jet on climate change on the Tibetan Plateau since the late Pleistocene, Quat. Sci. Rev., 163, 84-94, https://doi.org/10.1016/j.quascirev.2017.03.013, 2017a.

Hou, J., Huang, Y., Zhao, J., Liu, Z., Colman, S., and An, Z.: Large Holocene summer temperature oscillations and impact on the peopling of the northeastern Tibetan Plateau, Geophys. Res. Lett., 43, 1323-1330, https://doi.org/10.1002/2015GL067317, 2016.

Hou, J., Tian, Q., Liang, J., Wang, M., and He, Y.: Climatic implications of hydrologic changes in two lake catchments on the central Tibetan Plateau since the last glacial, J. Paleolimnol., 58, 257-273, https://doi.org/10.1007/s10933-017-9976-9, 2017b.

Hu, G., Yu, L., Dong, Z., Jin, H., Luo, D., Wang, Y., and Lai, Z.: Holocene aeolian activity in the Headwater Region of the Yellow River, Northeast Tibet Plateau, China: A first approach by using OSL-dating, Catena, 149, 150-157, https://doi.org/10.1016/j.catena.2016.09.014, 2017.

Hu, G., Yu, L., Dong, Z., Lu, J., Li, J., Wang, Y., and Lai, Z.: Holocene aeolian activity in the Zoige Basin, northeastern Tibetan Plateau, China, Catena, 160, 321-328, https://doi.org/10.1016/j.catena.2017.10.005, 2018.

Huang, E., Wang, P., Wang, Y., Yan, M., Tian, J., Li, S., and Ma, W.: Dole effect as a measurement of the low-latitude hydrological cycle over the past 800 ka, Sci. Adv., 6, eaba4823, https://doi.org/10.1126/sciadv.aba4823, 2020.

Huo, B. Y., Guo, B. H., Liu, C. Y., Xu, H. M., and Jiang, Y. Q.: Significance of surface

https://doi.org/10.5194/essd-2026-373
Preprint. Discussion started: 14 July 2026

soil magnetic susceptibility in the Tengger Desert, Arid Zone Res., 42, 613–621, https://doi.org/10.13866/j.azr.2025.04.04, 2025 (in Chinese).

Kasper, T., Haberzettl, T., Doberschutz, S., Daut, G., Wang, J., Zhu, L., Nowaczyk, N. R., and Mausbacher, R.: Indian ocean summer monsoon (IOSM)-dynamics within the past 4 ka recorded in the sediments of lake nam Co, central Tibetan plateau (China), Quat. Sci. Rev., 39, 73-85, https://doi.org/10.1016/j.quascirev.2012.02.011, 2012.

Lehmkuhl, F., Schulte, P., Zhao, H., Hülle, D., Protze, J., and Stauch, G.: Timing and spatial distribution of loess and loess-like sediments in the mountain areas of the northeastern Tibetan Plateau, Catena, 117, 23-33, https://doi.org/10.1016/j.catena.2013.06.008, 2014.

Li, Y., Shang, H., Yan, S., Zhang, Z., Gao, M., Liu, S., Xi, T., Zhao, J., and Sun, W.: The Integrated Multi-proxy Paleoclimate Database for the Northeastern Tibetan Plateau, Mendeley Data, https://doi.org/10.17632/cp7kftnb94.1, 2026.

Li, Y. and Morrill, C.: A holocene east asian winter monsoon record at the southern edge of the gobi desert and its comparison with a transient simulation, Clim. Dynam., 45, 1219-1234, https://doi.org/10.1007/s00382-014-2372-5, 2015.

Li, Y. and Peng, S.: Ecological and hydrologic evolution history in the sensitive zone of both east Asian summer monsoon and westerly since the last glacial maximum, J. Mountain Sci., 20, 1266–1281, https://doi.org/10.1007/s11629-022-7851-2, 2023.

Li, Y., Peng, S., Hao, L., Zhou, X., and Li, H.: Interactions of the westerlies and Asian summer monsoon since the last deglaciation in the northeastern Qinghai-Tibet Plateau, Paleoceanography and Paleoclimatology, 37, e2022PA004548, https://doi.org/10.1029/2022PA004548, 2022.

Li, Y., Zhang, Z., Gao, M., Duan, J., Xue, Y., Shang, H., and Liu, S.: Monsoon marginal zone's dry/wet status and their links with tropical ocean–atmosphere interactions during the holocene, Sci. Bull., https://doi.org/10.1016/j.scib.2025.03.057, 2025.

Liang, E., Shao, X., Eckstein, D., and Liu, X.: Spatial variability of tree growth along a latitudinal transect in the Qilian Mountains, northeastern Tibetan Plateau, Can. J. Forest Res., 40, 200-211, https://doi.org/10.1139/X09-186, 2010.

Lister, G. S., Kelts, K., Zao, C. K., Yu, J.-Q., and Niessen, F.: Lake Qinghai, China: closed-basin lake levels and the oxygen isotope record for ostracoda since the latest Pleistocene, Palaeogeogr. Palaeoclimatol. Palaeoecol., 84, 141-162, https://doi.org/10.1016/0031-0182(91)90041-O, 1991.

Liu, K.-B., Yao, Z., and Thompson, L. G.: A pollen record of Holocene climatic changes from the Dunde ice cap, Qinghai-Tibetan Plateau, Geology, 26, 135-138, https://doi.org/10.1130/0091-7613(1998)026<0135:APROHC>2.3.CO;2, 1998.

Liu, W., Li, X., An, Z., Xu, L., and Zhang, Q.: Total organic carbon isotopes: a novel proxy of lake level from Lake Qinghai in the Qinghai-Tibet Plateau, China, Chem. Geol., 347, 153-160, https://doi.org/10.1016/j.chemgeo.2013.04.009, 2013.

Liu, X., Dong, H., Yang, X., Herzschuh, U., Zhang, E., Stuut, J.-B. W., and Wang, Y.:

Late Holocene forcing of the Asian winter and summer monsoon as evidenced by proxy records from the northern Qinghai-Tibetan Plateau, Earth Planet. Sci. Lett., 280, 276-284, https://doi.org/10.1016/j.epsl.2009.01.041, 2009.
Liu, X., Herzschuh, U., Wang, Y., Kuhn, G., and Yu, Z.: Glacier fluctuations of Muztagh Ata and temperature changes during the late Holocene in westernmost Tibetan Plateau, based on glaciolacustrine sediment records, Geophys. Res. Lett., 41, 6265-6273, https://doi.org/10.1002/2014GL060444, 2014.
Liu, X., Shen, J., Wang, S., Wang, Y., and Liu, W.: Southwest monsoon changes indicated by oxygen isotope of ostracode shells from sediments in Qinghai Lake since the late Glacial, Chin. Sci. Bull., 52, 539-544, https://doi.org/10.1007/s11434-007-0086-3, 2007.
Liu, X. D., Cheng, Z. G., Yan, L. B., et al.: Elevation dependency of recent and future minimum surface air temperature trends in the Tibetan Plateau and its surroundings, Global Planet. Change, 68, 164-174, https://doi.org/10.1016/j.gloplacha.2009.03.017, 2009a.
Liu, X. J., Lai, Z. P., Madsen, D. B., and Zeng, F. M.: Last deglacial and Holocene lake level variations of Qinghai Lake, north-eastern Qinghai-Tibetan plateau, J. Quat. Sci., 30, 245-257, https://doi.org/10.1002/jqs.2777, 2015.
Liu, Y., Wang, Q., Ma, Z., Liu, X., and Yan, Y.: 540-year runoff reconstruction of upper Heihe River using tree-ring chronology, J. Arid Land Resour. Environ., 23, 93-97, https://doi.org/10.13448/j.cnki.jalre.2009.03.011, 2009b (in Chinese).
Lu, H., Wu, N., Liu, K.-B., Zhu, L., Yang, X., Yao, T., Wang, L., Li, Q., Liu, X., Shen, C., Li, X., Tong, G., and Jiang, H.: Modern pollen distributions in Qinghai-Tibetan Plateau and the development of transfer functions for reconstructing Holocene environmental changes, Quat. Sci. Rev., 30, 947-966, https://doi.org/10.1016/j.quascirev.2011.01.008, 2011.
Long, H., Zhang, J., Zhang, S., Hou, Y., Wu, Y., Yang, N., Zhang, C., Cheng, L., Zhao, Z., Cheng, J., and Shen, J.: The westerlies-monsoon interaction shaped asymmetric lake expansions over the Tibetan Plateau in warming periods, Sci. Bull., https://doi.org/10.1016/j.scib.2025.07.023, 2025.
Ma, Q., Zhu, L., Lü, X., Guo, Y., Ju, J., Wang, J., Wang, Y., and Tang, L.: Pollen-inferred Holocene vegetation and climate histories in Taro Co, southwestern Tibetan Plateau, Chin. Sci. Bull., 59, 4101-4114, https://doi.org/10.1007/s11434-014-0505-1, 2014.
PAGES 2k Consortium: A global multiproxy database for temperature reconstructions of the Common Era, Sci. Data, 4, 170088, https://doi.org/10.1038/sdata.2017.88, 2017.
Pan, B., Li, J., and Chen, F.: Qinghai-Tibetan Plateau: A driver and amplifier of global climate changes, J. Lanzhou Univ. (Nat. Sci.), 31, 120-128, https://doi.org/10.13885/j.issn.0455-2059.1995.03.024, 1995 (in Chinese).
Qie, J.-Z., Zhang, Y., Trappmann, D., Zhao, Y.-H., Ballesteros-Canovas, J. A., Favillier, A., and Stoffel, M.: Long-term reconstruction of flash floods in the Qilian Mountains, China, based on dendrogeomorphic methods, J. Mt. Sci., 19, 3163-3177, https://doi.org/10.1007/s11629-022-7577-1, 2022.

https://doi.org/10.5194/essd-2026-373
Preprint. Discussion started: 14 July 2026

Qiu, J.: China: the third pole, Nature, 454, 393-396, https://doi.org/10.1038/454393a, 2008.

Reimer, P. J., Austin, W. E. N., Bard, E., et al.: The IntCal20 Northern Hemisphere radiocarbon age calibration curve (0-55 cal kBP), Radiocarbon, 62, 725-757, https://doi.org/10.1017/RDC.2020.41, 2020.

Schiemann, R., Lüthi, D., and Schär, C.: Seasonality and interannual variability of the westerly jet in the Tibetan Plateau region, J. Climate, 22, 2940-2957, https://doi.org/10.1175/2008JCLI2625.1, 2009.

Shen, C., Liu, K. B., Morrill, C., Overpeck, J. T., Peng, J., and Tang, L.: Ecotone shift and major droughts during the mid-late Holocene in the central Tibetan Plateau, Ecology, 89, 1079-1088, https://doi.org/10.1890/06-2016.1, 2008.

Shi, F. F., Xiao, J. S., Li, L., Cao, X. Y., Li, X. D., Li, H. M.: A dataset of snow disaster grade monitoring based on meteorological elements in the pastoral area of the Tibetan Plateau, China Scientific Data, 7, 121–129, https://doi.org/10.11922/11-6035.ncdc.2021.0029.zh, 2022 (in Chinese).

Tang, L., Shen, C., Li, C., Peng, J., Liu, H., Liu, K.-B., Morrill, C., Overpeck, J. T., Cole, J. E., and Yang, B.: Pollen-inferred vegetation and environmental changes in the central Tibetan Plateau since 8200 yr BP, Sci. China Ser. D, 52, 1104-1114, https://doi.org/10.1007/s11430-009-0080-5, 2009.

Tang, L., Shen, C., Liao, G., and Overpeck, J. T.: New high-resolution pollen records from two lakes in Xizang (Tibet), Acta Bot. Sin., 41, 896-902, 1999.

Tang, L., Shen, C., Liu, K., and Overpeck, J. T.: Changes in South Asian monsoon: New high-resolution paleoclimatic records from Tibet, China, Chin. Sci. Bull., 45, 87-91, https://doi.org/10.1007/BF02884911, 2000.

Thompson, L. G., Yao, T., Davis, M. E., Henderson, K. A., Mosley-Thompson, E., Lin, P. N., Beer, J., Synal, H. A., Cole-Dai, J., and Bolzan, J. F.: Tropical climate instability: The last glacial cycle from a Qinghai-Tibetan ice core, Science, 276, 1821-1825, https://doi.org/10.1126/science.276.5320.1821, 1997.

Tian, L., Masson-Delmotte, V., Stievenard, M., Yao, T., and Jouzel, J.: Tibetan Plateau summer monsoon northward extent revealed by measurements of water stable isotopes, J. Geophys. Res.-Atmos., 106, 28081-28088, https://doi.org/10.1029/2001JD900186, 2001.

Wang, F. F., Hou, G. L., Hou, X. Q., and Wang, Q. B.: Researches on Climate Parameters for Quantitative Reconstruction Based on Surface Pollen in the Tibetan Plateau, Acta Geol. Sin., 38, 529–536, https://doi.org/10.3975/cagsb.2017.04.10, 2017 (in Chinese).

Wang, H., Dong, H., Zhang, C. L., Jiang, H., Zhao, M., Liu, Z., Lai, Z., and Liu, W.: Water depth affecting thaumarchaeol production in Lake Qinghai, northeastern Qinghai-Tibetan plateau: Implications for paleo lake levels and paleoclimate, Chem. Geol., 368, 76-84, https://doi.org/10.1016/j.chemgeo.2014.01.009, 2014.

Wang, N., Yao, T., Pu, J., Zhang, Y., and Sun, W.: Climatic and environmental changes during the past millennium recorded by the Malan ice core in the northern Tibetan Plateau, Sci. China Ser. D, 36, 723-732, https://doi.org/10.3321/j.issn:1006-9267.2006.08.005, 2006 (in Chinese).

Wang, S. Y., Wang, Q. L., Kang, S. C., Ding, Y. J., Xu, Y. A., and Huang, X. B.: Characteristics and controlling factors of stable isotopes in precipitation based on 9-year monitoring data in the monsoon transition zone of the Tibetan Plateau, Agric. For. Meteorol., https://doi.org/10.1016/j.agrformet.2025.110889, 2026.

Wu, D., Zhou, A., Zhang, J., Chen, J., Li, G., Wang, Q., Chen, L., Madsen, D., Abbott, M., Cheng, B., and Chen, F.: Temperature-induced dry climate in basins in the northeastern Tibetan Plateau during the early to middle Holocene, Quat. Sci. Rev., 237, 106311, https://doi.org/10.1016/j.quascirev.2020.106311, 2020.

Wu, G. X., Liu, Y. M., Liu, X., et al.: How the heating over the Tibetan Plateau affects the Asian climate in summer, Chin. J. Atmos. Sci., 29, 47-56, 2005 (in Chinese).

Wünnemann, B., Demske, D., Tarasov, P. E., Kotlia, B. S., Reinhardt, C., Bloemendal, J., Diekmann, B., Hartmann, K., Krois, J., and Riedel, F.: Hydrological evolution during the last 15 kyr in the Tso Kar lake basin (Ladakh, India), derived from geomorphological, sedimentological and palynological records, Quat. Sci. Rev., 29, 1138-1155, https://doi.org/10.1016/j.quascirev.2010.02.017, 2010.

Yang, B., He, M., Melvin, T. M., Osborn, T. J., and Briffa, K. R.: Climate control on tree growth at the upper and lower treelines: a case study in the Qilian Mountains, Tibetan Plateau, PLoS One, 8, e69065, https://doi.org/10.1371/journal.pone.0069065, 2013.

Yang, B., Qin, C., Shi, F., and Sonechkin, D. M.: Tree ring-based annual streamflow reconstruction for the Heihe River in arid northwestern China from AD 575 and its implications for water resource management, Holocene, 22, 773-784, https://doi.org/10.1177/0959683611430411, 2012.

Yang, B., Qin, C., Wang, J., He, M., Melvin, T. M., Osborn, T. J., and Briffa, K. R.: A 3,500-year tree-ring record of annual precipitation on the northeastern Tibetan Plateau, Proc. Natl. Acad. Sci., 111, 2903-2908, https://doi.org/10.1073/pnas.1319238111, 2014.

Yao, T., Thompson, L. G., Shi, Y., Qin, D., Jiao, K., Yang, Z., Tian, L., and Thompson, E. M.: Climate variation since the Last Interglaciation recorded in the Guliya ice core, Sci. China Ser. D, 40, 662-668, https://doi.org/10.1007/BF02877697, 1997.

Yin, Z.-Y., Zhu, H., Huang, L., and Shao, X.: Reconstruction of biological drought conditions during the past 2847 years in an alpine environment of the northeastern Tibetan Plateau, China, and possible linkages to solar forcing, Global Planet. Change, 143, 214-227, https://doi.org/10.1016/j.gloplacha.2016.04.010, 2016.

Zan, J. B., Ning, W. X., Yang, S. L., Fang, X. M., Kang, J., and Luo, Y. L.: Magnetic Variations in Surface Soils from the Tibetan Plateau and Its Adjacent Regions：Implications for Delineating the Climatic Boundary, Adv. Earth Sci., 37, 14–25, https://doi.org/10.11867/j.issn.1001-8166.2021.125, 2022 (in Chinese).

Zhan, S., Wang, K., Zhang, L., et al.: Species-specific growth responses to climatic factors in the eastern Qilian Mountains, Chin. J. Ecol., 38, 2007-2014, https://doi.org/10.13292/j.1000-4890.201907.021, 2019 (in Chinese).

Zhang, P. X., Zhang, B. Z., Qian, G. M., Li, H. J., and Xu, L. M.: The study of paleoclimatic parameter of Qinghai Lake since Holocene, Quat. Sci., 3, 225-236,

https://doi.org/10.5194/essd-2026-373
Preprint. Discussion started: 14 July 2026

1994 (in Chinese).

Zhang, Y., Shao, X. M., Yin, Z.-Y., and Wang, Y.: Millennial minimum temperature variations in the Qilian Mountains, China: evidence from tree rings, Clim. Past, 10, 1763-1778, https://doi.org/10.5194/cp-10-1763-2014, 2014.